Journal of Engineering Science and Technology
Vol. 18, No. 6 (2023) 2809 - 2822

NUMERICAL DEVELOPING THE INTERNET OF THINGS TO REMOTELY MONITOR THE PERFORMANCE OF A THREE DIMENSIONS PRINTER FOR FREE-FORM SURFACE

MOSTAFA A. ABDULLAH*, TAHSEEN F. ABBAS

Production Engineering and Metallurgy Department,
University of Technology- Iraq, Baghdad, Iraq
*Corresponding Author: mostafa.a.hamed@uotechnology.edu.iq

Abstract

Under the IR 4.0 concept, manufacturing processes will be pushed to become increasingly interconnected and require more efficiency. The Internet of Things (IoT) and 3D printing are two important modern technologies that are gradually affecting many industries and our daily lives to solve complex engineering problems. An Internet of Things (IoT) application allows 3D printers to be controlled and monitored by remote sensing and object control. The current study aims to design and develop an Internet of Things application to remotely monitor the performance of a 3D printer, including printing progress, table temperature, extruder temperatures, monitoring the printer during work, and monitoring the work progress by creating a low-cost real-time 3D printing parameter control system, remote-loading new prints, and monitoring extruder temperature by starting and stopping the printer, checking its progress, and watching it live. The IoT-based OctoPrint manages the 3D printers online. The system's performance was evaluated by printing free 3D surfaces and examining them to determine their conformity with the designs. The proposed method successfully served the purpose of real-time monitoring of the 3D printing process. The experimental work is to develop and build a multi-patched Bezier free-form surface. The model has been developed to represent the surface. Finally, during the measurement using CMM inspection, it was found that the beginning error of Family 1 was 0.230, for Family 11, it was 0.681, and the average percentage error was 0.159 for the face part.

Keywords: 3D-printing, Coordinate measuring machine, G-code, OctoPrint, Remote control system.

1. Introduction

A remote-control system is a prototype initially created using a 3D CAD design system and can be manufactured directly from layer to layer by Dhawale et al. [1]. Budzik et al. [2] developed a technical test for dimensional accuracy and surface roughness using ABS-M30, PLA, ABS, PETG, and PolyJet process models that measured internal and external thread profiles. It was found that the ABS-M30 has better surface quality than the PLA, ABS, and PETG 3D printers. Ali et al. [3] FDM-produced ABS components are affected by specimen tensile and compressive behaviour. Ultimaker+2 printers print ABS thermoplastic samples. Plastic experiments employ infill density, layer thickness, and pattern. Cross, zigzag, and gyroid specimens were tensile and compressive tested. A sample with 60% infill density, 0.05 mm layer thickness, and a GYROID infill pattern achieved maximum compressive strength at break (25.01 MPa). Tasneem et al. [4] developed a design. 3D printers use BLDC motors because their accuracy and efficiency are much higher than those of stepper motors. In addition, they use a ball screw instead of the main screw, as it provides smoother, quieter, and more efficient movement. Dhawale et al. [5] studied quickly made prototypes of cases or packages for custom IoT-enabled sensors. The authors also discussed the parameters' utilization, like the used nozzle sizes of 0.4 mm and 0.6 mm.

ABS is another material choice, although it is more costly and more difficult to print than PLA. Components for the 3D-printed enclosure design for the IoT-enabled sensor were created. The 0.6-mm nozzle is based on RF and Wi-Fi. Brion and Pattinson [6] instructed a multi-head neural network with photos that have been automatically labelled based on how far they are from the best settings for printing. Automating data collection and labelling makes it possible to create a training image-based dataset that is big enough and varied enough to find errors. 1.2 million images from 192 different parts labelled with the printing parameters and printers can be found in real-time and fixed quickly. Jasim et al. [7] investigated the effect of polylactic acid (PLA) test specimens' tensile strength on many infill patterns. By utilizing the subdivision using ten different infill patterns (grid, zigzag, octet triangles, tri-hexagon, cubic, gyroid, and cube), the tensile strength of the concentric infill design was 32.174 MPa. In contrast, the tensile strength of the triangular infill pattern was just 20.934 MPa.

Shinde et al. [8] stated that Internet of Things (IoT)-based 3D printers can be operated or controlled using the Internet. The Raspberry Pi connects users and 3D printers over the Internet. Octo-Print is a software package that runs on the Raspberry Pi. The results of the movement accuracy test revealed that there isn't a significant difference between the input value and the measured value. Abbas et al. [9] aimed to control 3D printer parts from a distance. IoT is the foundation of the system. Wireless 3D printers are better in many ways than those that use cables. There is no longer a need for an SD card to move the information from the computer to the 3D printer. The research of Yi et al. [10] is a step toward improving the multipurpose FDM technique for ABS prints. The effects of four major FDM factors, including infill density, outer shell width, infill pattern, and layer thickness, were investigated at various degrees of each parameter. The results showed that raising the infill's density increases the material's mass per unit volume if the proper infill pattern is used.

Pernet et al. [11] examined mechanical behaviours, economic benefits, and environmental impacts of infill patterns using compression tests, life cycle cost assessment, and life cycle assessment. Fourteen infill patterns were tested at different densities, with 80% or 100% densities, and the better infill pattern was concentric, being more efficient. Jang et al. [12] proposed a quality management system to ensure the safety of low-cost and expensive 3D printers and finished products. It designs IoT beacon-based remote safety systems for individual users, addressing shrinkage problems and unstable output situations. The system monitors and controls the output environment in real-time, preventing errors, fires, and defects and ensuring the best quality output for long-term operation. Sunny et al. [13] used a 3DP-FAS system to remotely control, monitor, and analyse 3D printing processes using a camera module and fine-tuned models. It makes intelligent decisions based on analysis and offers a web-based monitoring interface. The IoT Cloud Research Laboratory experimented with the system, combining IoT with 3D printing for Industry 4.0. Fatima et al. [14] explored the potential of 3D printing and IoT in the medical industry, highlighting the importance of selecting the right materials for tissue creation and medical emergencies. Combining these technologies can speed up and improve medical emergencies while addressing the needs of cranial and maxillofacial structures. Materials like hydrogels, fibrin, and titanium suit various medical requirements, making material selection a critical component of medical practices.

This study explores a low-cost, real-time 3D printing parameter control system, remote printing, and monitoring extruder temperature. OctoPrint manages online 3D printers, eliminating SD cards for data transfer. Remote printing was used to create dental coverings using PLA material for problematic cases.

2. Materials and Methods

The current research describes developing a low-cost, real-time 3D printing parameter control system, remotely loading fresh prints, keeping track of extruder temperature while starting and stopping the printer, checking its status, and seeing it live. The IoT-based OctoPrint handles online 3D printer management. There are no more SD cards for PC-to-3D printer data transfer. Printing is done remotely. This method was applied to manufacture dental covers based on PLA material for pathological cases, and good results were achieved.

2.1. Remote control system

A Raspberry Pi computer prints models from a remote and keeps a watch on every part of the 3D printer. The most advantageous use of information technology is discussed with the printer through a hardwired USB connection. The traditional printing method (with a cable or SD card) isn't as good as a wireless 3D printer. The layout of the developed system is shown in Fig. 1.

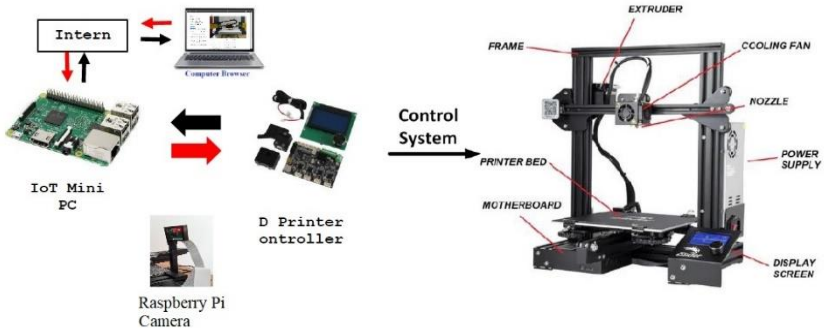

Fig. 1. The developed control system for remote printing.

2.2. System architectural

The system block diagram is depicted in Fig. 2. The central core of the system is the Raspberry Pi 4 with built-in Wi-Fi. It is the host of OctoPrint, which controls the 3D printer and collects the temperatures of the heated bed and hot end. for the 3D printer board (RAM Bo 1.2G) and the webcam (Logitech C170). Using OctoPrint software allows access to the printer within a browser, through which the user can monitor each step from another PC and a smartphone.

The key aspects of this software are:

- Complete control over the printer, axis movement, tool temperature, extruder behaviour, etc.
- Live printing view.
- Start, pause, continue, and stop 3D printing.
- Code-based serial 3D printer communication.
- Time-lapse printing mistake detection.

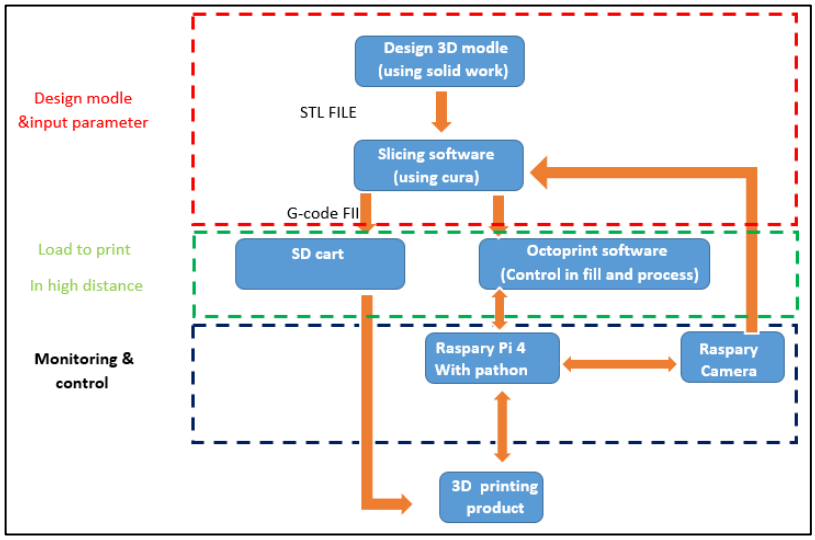

Fig. 2. Software structure of the remote-control system.

Next, for building, heating the bed, moving the head or the extruder by directly talking to the stepper motors, and tasks like preparing the printing file is also included. This makes it possible to directly download the STL file of an externally created 3D model and get it sliced by the Cura program, as shown in Fig. 3. Table 1 shows the parameters of the 3D printer used in the experimental work.

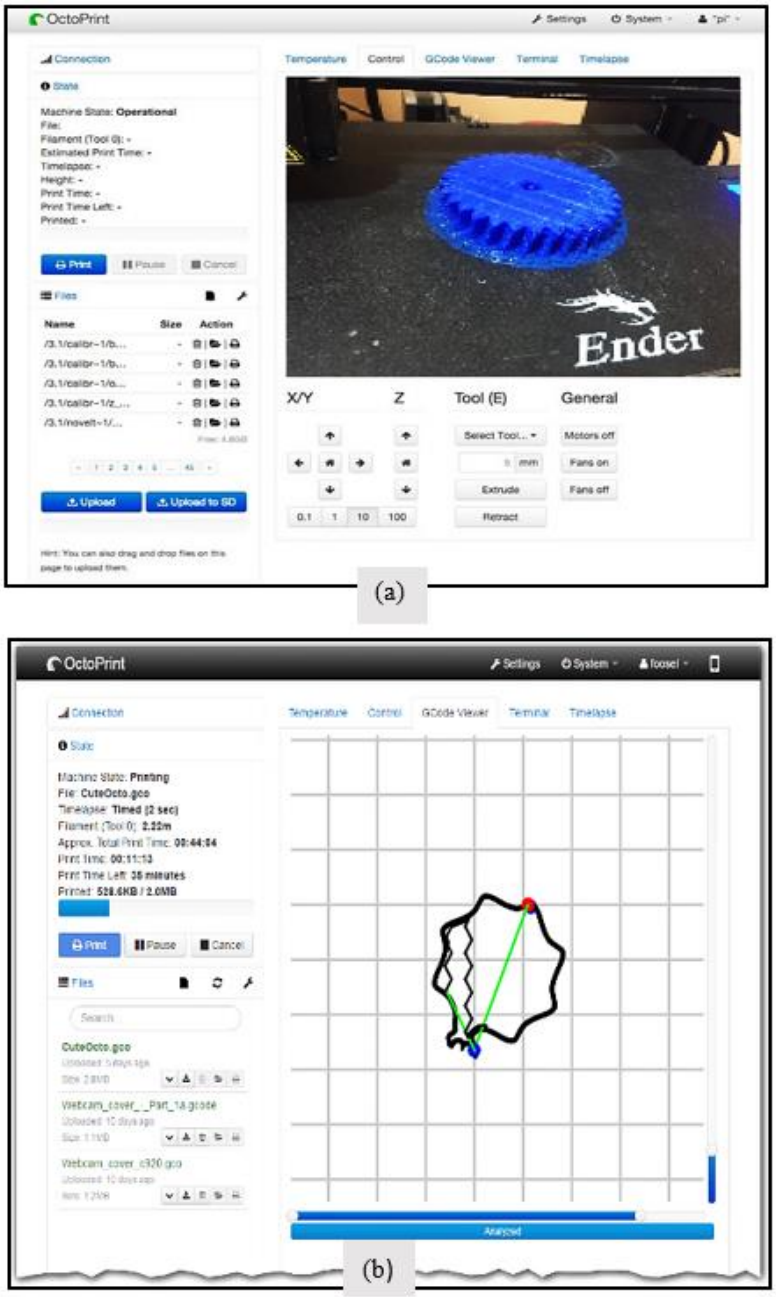

Fig. 3. The face OctoPrint program interface.

Table 1. Test model specifications and test conditions.

Parameters	Value	Units
Printing speed	60	mm/s
Infill density	80	%
Printing temperature	200	Degree Celsius
Shell wall thickness	1	mm
Layer thickness	0.1	mm
Build plate temperature	50	Degree Celsius

2.3. Risks by the electronics and coming along risks by external parts of 3D printing.

The actual risks due to the system and its environment are a danger to people's health, and the following policies should be taken seriously even if the actual motivation of an attacker is not considered a common failure. The risks can range from a destroyed print to a high fire hazard. An overview of the main risks is summarized as follows by Prianto et al. [15]:

- Modifications or destruction of the current print job.
- Harm to the printer by mechanical deformations: analysis of commonly used stop-end printing.
- Heating elements pose fire hazards.

2.4. Free-form surface

Free-form surface reconstruction converts a point cloud or a polygonal mesh into an analytical surface that may be represented as a parametric equation. The target surface fitting represents measurable points with a continuous model. The surface reconstruction involves interpolation and approximation. The interpolated surfaces pass via the measured point, whereas the approximated surfaces pass near the points [1, 2]. Surface reconstruction is essential for converting point clouds to CAD formats. For Bezier surface patches like Bezier curves as approximately free-form surfaces, the Bezier patch matrix equation is:

$$P(u,w) = U_{1,n} M_{B,n,n} P_{n,m} M^{T}_{B,m,m} {W^{T}}_{m,1} \tag{1}$$

2.5. Derivative of the proposed Bezier matrix

Bezier representation was used for this work due to its appealing characteristics. For a Bernstein-driven six-degree surface, the matrix shape is:

$$\begin{aligned} U &= [u^6 \quad u^5 \quad u^4 \quad u^3 \quad u^2 \quad u \quad 1], \\ P &= [p_\circ \quad p_1 \quad p_2 \quad p_3 \quad p_4 \quad p_5 \quad p_6]^T \end{aligned} \tag{2}$$

$$M_{\mathrm{B}(6)} = \begin{bmatrix} 1 & -6 & 15 & -20 & 15 & -6 & 1 \\ -6 & 30 & -60 & 60 & -30 & 6 & 0 \\ 15 & -60 & 90 & -60 & 15 & 0 & 0 \\ -20 & 60 & -60 & 20 & 0 & 0 & 0 \\ 15 & -30 & 15 & 0 & 0 & 0 & 0 \\ -6 & 6 & 0 & 0 & 0 & 0 & 0 \\ 1 & 0 & 0 & 0 & 0 & 0 & 0 \end{bmatrix} \tag{3}$$

2.6. Design and implementation

CAD/CAM modules in computers create and reconstruct surfaces, produce offset models, process offset surfaces to generate tool paths, and post-process tool paths to generate MATLAB, UG-NX8, and CIMCO Edit. These programs were used to complete these projects on personal PCs.

2.7. MATLAB software

In the MATLAB-Math Works' numerical computing environment, MATLAB can plot functions, manipulate matrices, and construct algorithms. This application builds algorithms using a basis function matrix to construct diverse Bezier surfaces. This program has no direct Bezier surface creation capability. Hence, special subroutines create Bezier or multi-patched Bezier surfaces by Woźniak and Męczyńska [16].

2.8. UG-NX8 software

Unigraphics (UG-NX) is Siemens Software PLM's CAD/CAM software. Among other things, it manages integrated design, analytical engineering, and design and machining. UG-NX provides a fully integrated tool for simulations and validations of the complete cutting process, including the dynamic materials removed by Sang et al. [17].

2.9. Transferring CAD data to CAM module

The CAD modules describe the profile of the curves creating the surfaces in MATLAB and transfer them to UGS-NX8 via TXT data exchanges to observe the desired shape. Figure 6 manifests the iso-parametric conversion surface into a series of curves. Each matrix is exported to UG-NX8 as a text file. The processes described above are shown in Figs. 4 to 7.

Insert curve → *Spline curve* → *Through points* → *Points from file.*

Insert Surface → *Mesh surface* → *Through curves*

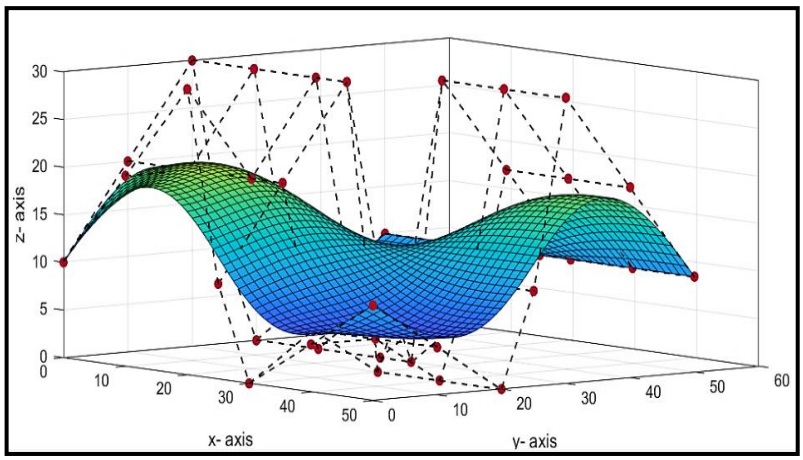

Fig. 4. Surface digitization scheme in the MATLAB environment.

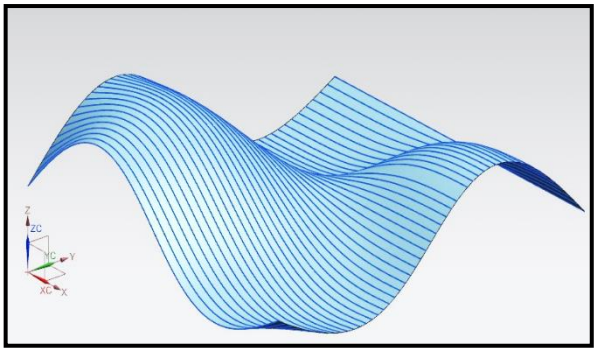

Fig. 5. Imported surface, which is ready for the manufacturing process.

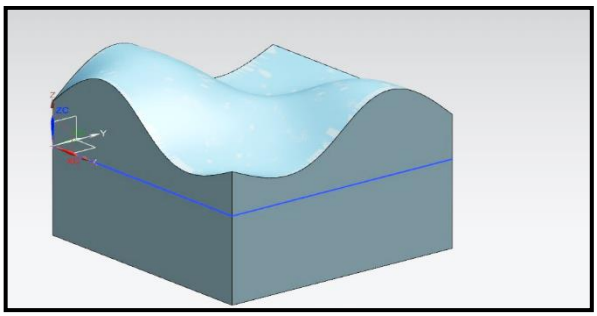

Fig. 6. The machined planes of the reference point.

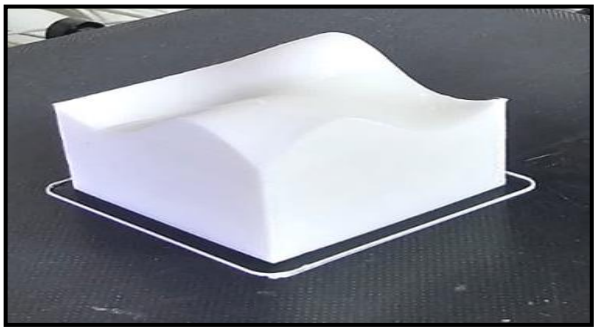

Fig. 7. Solid body by extruding a surface for 3D printing.

2.10. CMM inspection

The portable CMM, shown in Fig. 8, performs three-dimensional inspections, tool certifications, dimensional analysis, CAD comparison, and reverse engineering to help producers verify product quality.

Table 2 presents the part measurement data. A CMM examination between the CAD model and the physical part improves the measurement accuracy. This procedure requires machining the planes regarded as the origin point, and one of the main measurement steps is defining the reference point planes by passing the probe on each plane. The points define that plane. Machining these planes will help fix the points accurately and match the CAD model and the real part. Figure 9

portrays the reference point machined planes. The average percentage error in table 2 is equal to 1.973.

Fig. 8. Portable CMM.

Table 2. Sample of measurement data for the face part.

C1R11	C2R11	C3R11	C4R11	C5R11	C6R11	C7R11	C8R11	C9R11	C10R11	C11R11	Family 11	4.871
C1R10	C2R10	C3R10	C4R10	C5R10	C6R10	C7R10	C8R10	C9R10	C10R10	C11R10	Family 10	13.812
C1R9	C2R9	C3R9	C4R9	C5R9	C6R9	C7R9	C8R9	C9R9	C10R9	C11R9	Family 9	3.129
C1R8	C2R8	C3R8	C4R8	C5R8	C6R8	C7R8	C8R8	C9R8	C10R8	C11R8	Family 8	13.721
C1R7	C2R7	C3R7	C4R7	C5R7	C6R7	C7R7	C8R7	C9R7	C10R7	C11R7	Family7	0.505
C1R6	C2R6	C3R6	C4R6	C5R6	C6R6	C7R6	C8R6	C9R6	C10R6	C11R6	Family 6	9.957
C1R5	C2R5	C3R5	C4R5	C5R5	C6R5	C7R5	C8R5	C9R5	C10R5	C11R5	Family 5	10.014
C1R4	C2R4	C3R4	C4R4	C5R4	C6R4	C7R4	C8R4	C9R4	C10R4	C11R4	Family 4	1.636
C1R3	C2R3	C3R3	C4R3	C5R3	C6R3	C7R3	C8R3	C9R3	C10R3	C11R3	Family 3	9.770
C1R2	C2R2	C3R2	C4R2	C5R2	C6R2	C7R2	C8R2	C9R2	C10R2	C11R2	Family 2	1.210
C1R1	C2R1	C3R1	C4R1	C5R1	C6R1	C7R1	C8R1	C9R1	C10R1	C11R1	Family 1	5.742

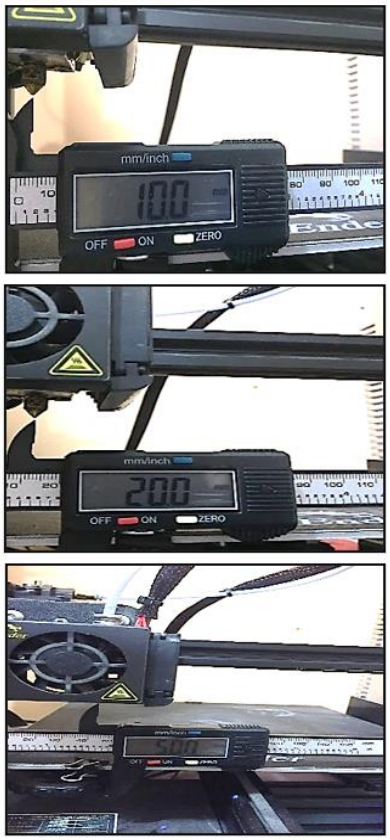

Fig. 9. 3D printer nozzle movement measurement.

3. Experimental Results

3.1. Performance of the IoT system

An IoT-based 3D printer was evaluated for accuracy by supplying input commands through devices (mobile phones and laptops), monitoring, and comparing the command and machine movement in the X, Y, or Z axes that move the nozzle toward the specified axis. After measuring the movement using Vernier, the output and instruction are compared (input), as displayed in Fig. 4 and Table 3. The result of Table 3 reveals that the input and measured values for nozzle movement along the X, Y, and Z axes are similar. Implementation testing employed polylactic acid filaments (PLA).

Table 3. comparing the command and machine movement in the X, Y, or Z axes.

Z-axis position (mm)		Y-Axis Position (mm)		X-axis position (mm)	
Measured Value	**Input**	**Measured Value**	**Input**	**Measured Value**	**Input**
10	0-10	10	0-10	10	0-10
10	10-20	10	10-20	10	10-20
10	20-30	10	20-30	10	20-30
10	30-40	10	30-40	10	30-40
10	50-60	10	50-60	10	50-60
10	60-70	10	60-70	10	60-70
10	70-80	10	70-80	10	70-80
10	80-90	10	80-90	10	80-90
10	90-10	10	90-10	10	90-10

3.2. Extruder calibration temperature

Extruder temperature calibration is a simple procedure that keeps the 3D printer head and bed temperature constant, regulating fluctuations. This is a matter of the density of the filament material and the difference in viscosity at different temperatures. At a lower temperature, the viscosity of the filament may be slightly higher, while at a higher temperature, the 3D printer filament may be slightly more fluid. With layers of 0.1-0.2 mm and small heads, e.g., 0.1 mm, they may have some effects. The OctoPrint temperature tab suggests entering 40 °C in the "Tool" temperature box. The extruder temperature in the graph should start to increase (within about 30 seconds or so). This plugin replaces the default temperature tab of OctoPrint with a plotly.js graph and data by equality between the measured and actual temperature that incorporates other data supplied, as displayed in Fig. 10.

(a) Interface of OctoPrint temperature chart for measured and actual temperatures (bed and extruder).

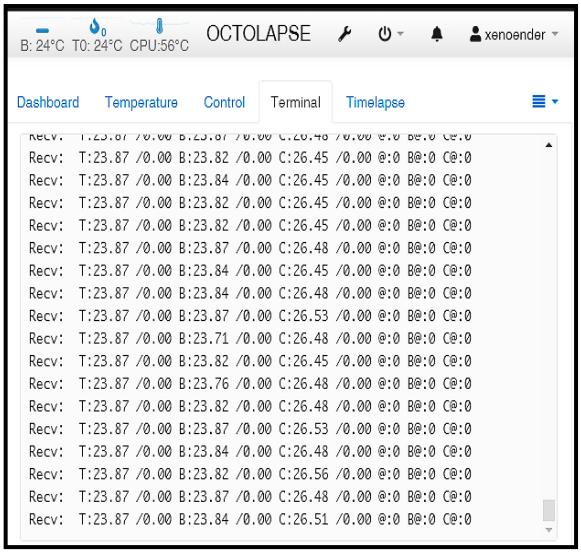

(b) Interface of OctoPrint temperature data for measured and actual temperatures (bed and extruder).

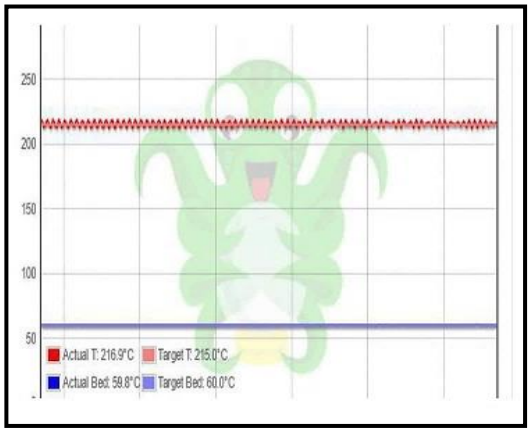

(c) Zoom Interface of OctoPrint temperature chart.

Fig. 10. The measured and actual temperatures.

4. Discussion

Figure 11 shows the relationship between the points generated for the surface (z-axis) by the MATLAB program (CAD design) and the points that were measured by the CMM device for the practical part. The results showed an increase in the values of the (z) axis over the designed values, i.e., an increase in the (z) axis. manufactured by a 3D printer. This is due to the finish of the manufactured surface, or the material used in the product, as it is a plastic material without additives to strengthen it, such as carbon or glass fibres, which give stability and a good finish to the product. The result compares CAD and experimental points, as illustrated in Fig. 12.

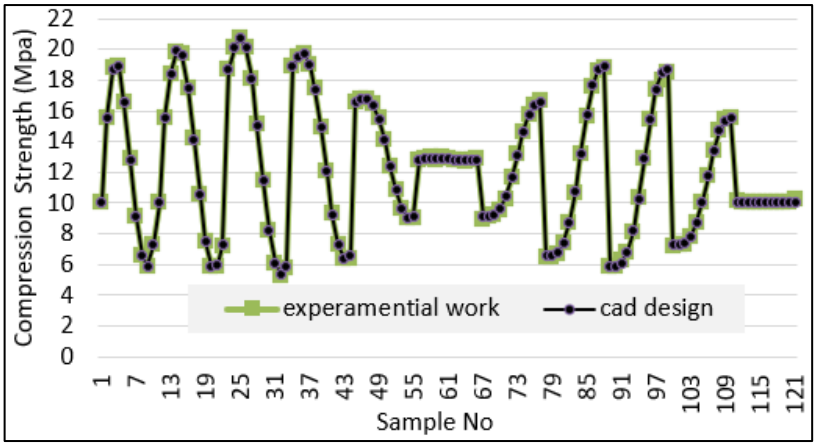

Fig. 11. Free form surface experimental work and cad design.

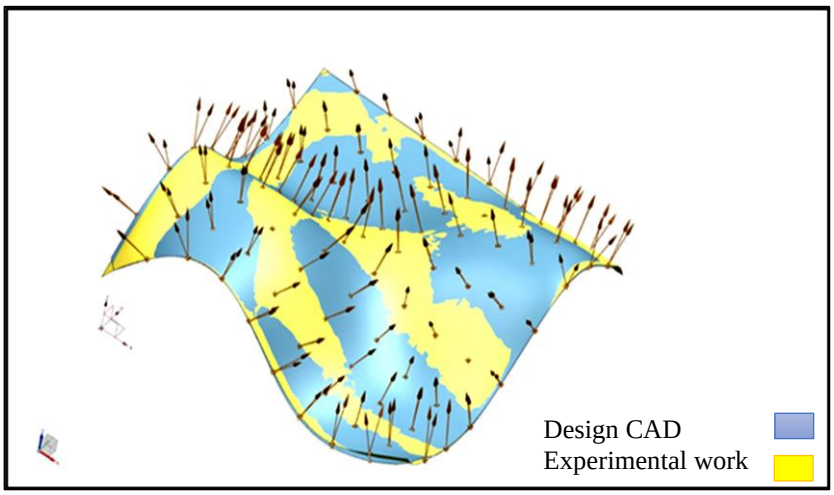

Fig. 12. Comparison of the cad point with the experimental points.

5. Conclusions

This study describes converting a virtual 3D model into a physical object. A fused deposition is a manufacturing method where layers of materials are built up to create a solid object. This study's main goal is to remotely control aspects of 3D printers. A wireless 3D printer has several advantages over a traditional wired setup. One no longer needs to use an SD card to copy files from the computer to the 3D printer. It enables remote wireless printing. Multi-patches Bezier surface construction and manufacture using MATLAB software determined the average percentage error (0.159), maximum error (0.986) mm, and minimum error (-1.100) mm for the cross-sectional surface. There are various potential areas for future research, including:

- Adapting the OctoPrint plugin for Mac IOS.
- Extending the scheduler's compatibility beyond Linux, the major operating system utilized during project development.

- Simplifying the process of managing many printers within OctoPrint, which is currently complex.
- Resolving problems that cause checksum errors and prevent some prints from finishing, wasting time and resources.
- OctoPrint is being translated into new languages.
- Increasing login security, especially for external access to OctoPrint servers.

Nomenclature

$B(u, i)$	The foundation function or blending function for u. An influence or weight of a control point in the u direction.
M	Blending a function matrix in u. (n+1) x 1 are its dimensions.
M^T	Transpose the blending functions matrix M. Matrix size is 1 x (n+1).
M	The v-direction Bézier patch degree. The number of v-direction control points and matrix G rows are determined.
N	The u-direction Bézier patch degree. The number of u-direction control points and matrix G size are determined.
$P(i, j)$	The Bézier patch's control point is index (i, j). These points shape the patch.
$P(u, v)$	A point's Bézier patch position at parametric values u and v.
p	Control point matrix. The dimensions are (m+1) x (n+1).
$P(i, j)$	The Bézier patch's control point is index (i, j). These points shape the patch.

References

1. Dhawale, N.M.; Patil, S.A.; Rajput, A.R.; Shinde, K.A.; Kulkarni, R.S.; and Chavan, N.R. (2021). On design rapid prototyping and testing of IOT enabled sensors using open-source tools. *International Journal of Advances in Engineering and Management*, 3(10), 168-173.
2. Budzik, G.; Dziubek, T.; Kawalec, A.; Turek, P.; Bazan, A.; Dębski, M.; Józwik, J.; Poliński, P.; Kiełbicki, M.; Kochmański, Ł.; Oleksy, M.; Cebulski, J.; Paszkiewicz, A.; and Kuric, I. (2023). Geometrical accuracy of threaded elements manufacture by 3D printing process. *Advances in Science and Technology Research Journal*, 17(1), 35-45.
3. Ali, H.B.; Oleiwi, J.K.; and Othman, F.M. (2022). Compressive and tensile properties of abs material as a function of 3D printing process parameters. *Revue Des Composites et Des Materiaux Avances*, 32(3), 117-123.
4. Bin Tasneem, M.H.B; and Amer, G.T. (2019). Design, fabrication and testing of a 3d printer. *Proceedings of the International Conference on Industrial Engineering and Operations Management*. Pilsen, Czech Republic, 2334-2344.
5. Dhawale, N.M.; Ghewade, D.V.; Patil, S.S.; Gangatirkar, R.S.; and Inamdar, N.A. (2022). An application of 3D printing technology for rapid prototyping of an IOT enabled sensor enclosure. *International Journal of Innovative Research in Science Engineering and Technology*, 11(2).

6. Brion, D.A.J.; and Pattinson, S.W. (2022). Generalisable 3D printing error detection and correction via multi-head neural networks. *Nature Communications*, 13(1), 4654.
7. Jasim, M.; Abbas, T.; and Huayier, A. (2022). The effect of infill pattern on tensile strength of PLA material in fused deposition modeling (FDM) process. *Engineering and Technology Journal*, 40(12), 1723-1730.
8. Shinde, Y.; Madaki, R.; and Nadaf, S. (2008). IoT-based 3D printer. *International Research Journal of Engineering and Technology*, 6(4), 1015-1020.
9. Abbas, T.F.; Mansor, K.K.; and Ali, H.B. (2022). The effect of FDM process parameters on the compressive property of ABS prints. *Journal of Hunan University Natural Sciences*, 49(7), 154-162.
10. Yi, B.; Liang, R.; Wang, X.; Wu, S.; and Huang, N. (2022). Free-form surface form error evaluation based on smaller-scale sampling points in touch-trigger probing. *Precision Engineering*, 76, 255-260.
11. Pernet, B.; Nagel, J.K.; and Zhang, H. (2022). Compressive strength assessment of 3D printing infill patterns. *Procedia CIRP*, 105, 682-687.
12. Jang, D.-S.; Lee, H.-S.; and Oh, J.-C. (2020). IoT 3D printer design of individual 3D printer remote safety and quality management system based on IoT Beacon. *The Journal of the Korea Institute of Electronic Communication Sciences*, 15(2), 225-230.
13. Sunny, B.C.; Benedict, S.; and Keerthana, B. (2021). 3DP-FAS: An intelligent quality assurance system for 3D printer. *Proceedings of ACM/CSI/IEEECS Research & Industry Symposium on IoT Cloud for Societal Applications (IoTCloud* 21), 32-36.
14. Fatima, S.; Haleem, A.; Bahl, S.; Javaid, M.; Mahla, S. K.; and Singh, S. (2021). Exploring the significant applications of the internet of things (IoT) with 3D printing using advanced materials in medical field. *Materials Today: Proceedings*, 45(Part 6), 4844-4851.
15. Prianto, E.; Pramono, H.S.; and Yuchofif. (2021). IoT-based 3D printer development for student competence improvement. *Journal of Physics: Conference Series*, 2111(1): 012002.
16. Woźniak, A.; and Męczyńska, K. (2020). Measurement hysteresis of touch-trigger probes for CNC machine tools. *Measurement*, 156, 107568.
17. Sang, Y.; Yan, Y.; Yao, C.; and He, G. (2021). A new scanning lines distribution strategy for the form error evaluation of freeform surface on CMM. *Measurement*, 181, 109578.